HHS Public Access

Author manuscript

Trends Biochem Sci. Author manuscript; available in PMC 2022 July 15.

Published in final edited form as:

Trends Biochem Sci. 2020 September ; 45(9): 806–819. doi:10.1016/j.tibs.2020.05.008.

Current view of ligand and lipid recognition by the menthol receptor TRPM8

Ying Yin,

Seok-Yong Lee*

Department of Biochemistry, Duke University School of Medicine, Durham, North Carolina, 27710, USA.

Abstract

Transient receptor potential melastatin member 8 (TRPM8), which is a calcium-permeable ion channel, functions as the primary molecular sensor of cold and menthol in humans. Recent cryo-electron microscopy (cryo-EM) studies of TRPM8 have shown distinct structural features in its architecture and domain assembly compared to the capsaicin receptor TRPV1. Moreover, ligand bound TRPM8 structures have uncovered unforeseen binding sites for both cooling agonists and membrane lipid phosphatidylinositol 4,5-bisphosphate [$PI(4,5)P_2$]. These complex structures unveil the molecular basis of cooling agonist sensing by TRPM8 and the allosteric role of $PI(4,5)P_2$ in agonist binding for TRPM8 activation. Here, we review the recent advances in TRPM8 structural biology and investigate the molecular principles governing the distinguishing role of TRPM8 as the evolutionarily conserved menthol receptor.

Keywords

transient receptor potential ion channels; menthol receptor; cold receptor; cooling agent; $PI(4,5)P_2$ regulation; allosteric coupling

The molecular sensors of menthol and capsaicin in humans

The transient receptor potential (TRP) ion channel superfamily consists of calcium-permeable ion channels that serve diverse sensory physiological roles involved in vision, taste, touch, hearing, osmo- and thermo-sensation, etc. [1–3]. Among all TRP channels, TRPM8 and TRPV1 are two unique ion channels because they are responsible for not only cold and heat temperature sensation, respectively, but also chemically-induced cooling or burning sensations [4–8].

TRPM8, also known as the cold and menthol receptor 1 (CMR1), is the principal molecular detector of cold in humans and can be activated by innocuous cool to cold temperatures

*Correspondence to: S.-Y. Lee, seok-yong.lee@duke.edu, telephone: 919-684-1005.

below 28 °C [7, 8], and studies of TRPM8 knockout mice showed that the channel is required for cold sensing [9–11]. TRPM8 is also activated by **menthol** (see Glossary) and other chemical cooling agents, such as the menthol analog WS-12 and the super cooling **agonist** icilin [12–14]. Intriguingly, TRPM8 activation by cold and menthol requires the signaling phospholipid **phosphatidylinositol 4,5-bisphosphate** [**$PI(4,5)P_2$**] as depletion of $PI(4,5)P_2$ results in channel **desensitization** [15–17]. In contrast, TRPV1 is a noxious heat-sensitive ion channel with an activation thermal threshold of 42 °C and is activated by vanilloid compounds [i.e. **capsaicin** and resiniferatoxin (RTx)] and a spider toxin named the double-knot toxin (DkTx) [6, 18].

Since the *trpm8* and *trpv1* genes were cloned, many studies have been done to understand the mechanisms by which TRPM8 and TRPV1 can integrate chemical (cooling agents or vanilloids) and physical (temperature changes) stimuli into human sensation [19–22]. In particular, the search for molecular determinants that govern the cooling agent (e.g. menthol) sensitivity in TRPM8 and the vanilloid (e.g. capsaicin) sensitivity in TRPV1 has been an intense subject of the field, as menthol and capsaicin have been important tools to study sensory biology, and mechanistic understanding of cooling agonists or vanilloid dependent gating of TRPM8 or TRPV1 holds promises for future analgesic development targeting these ion channels [18, 23–31]. Therefore, here we will focus on the current structural insights into ligand recognition and channel gating of TRPM8 and TRPV1 channels, while the mechanistic understanding of temperature sensation is still in infancy. Based on structural comparisons with TRPV1 and other TRPM channels, we will also investigate and highlight the molecular determinants underlying the distinguishing role of TRPM8 channel as the evolutionarily conserved menthol receptor.

Structure determination of TRPM8 and TRPV1 channels

From an evolutionary standpoint, TRPM8 and TRPV1 show different degrees of conservation in the channel sensitivity to its own natural agonists. For instance, TRPM8 shows conserved sensitivity to the naturally occurring cooling agonist menthol across various species, including the less cold-sensitive hibernator animals [32, 33]. In contrast, mammalian TRPV1 are sensitive to capsaicin, while avian TRPV1 are not [34, 35]. Moreover, the capsaicin sensitivity in TRPV1 can be conferred to the TRPV2 channel, which is closely related to TRPV1, by introducing four mutations into the transmembrane domain [36, 37], whereas the efforts to transfer the menthol sensitivity of TRPM8 to other TRPM channels by chimeric studies have not been successful [38, 39].

To advance the mechanistic understandings of the ligand-dependent channel activation of TRPM8 and TRPV1, structural characterizations are highly demanded. In 2013, the determination of rat TRPV1 channel structures at near-atomic resolution using single-particle cryo-electron microscopy (cryo-EM) marked a breakthrough in the TRP channel structural biology field. Two accompanying papers reported three TRPV1 structures in the absence of ligand (TRPV1-Apo), in the presence of capsaicin (TRPV1-Capsaicin), and in the presence of both DkTx and RTx (TRPV1-DkTx/RTx) [40, 41]. Comparison of the TRPV1 structures suggested the mechanism of channel activation was characterized by dilation of the selectivity filter and a gate formed by a constriction point in the C-terminal

half of the transmembrane helices S6. A follow-up cryo-EM study of TRPV1 in 2016 [42], in which the purified channel protein was reconstituted into **nanodiscs**, revealed the regulatory roles of phospholipid in TRPV1 channel gating ($TRPV1_{ND}$-Apo and $TRPV1_{ND}$-DkTx/RTx).

In contrast to the ample structural information available for TRPV1, the architecture of TRPM8 channel remained unknown until the first cryo-EM structure of a collared flycatcher (*Ficedula albicollis*) TRPM8 channel in the apo conformation ($TRPM8_{FA}$-Apo) was published in 2017 [43], which revealed novel structural motifs and extensive domain organizations in TRPM8 distinct from previously reported TRP channels. In early 2019, structures of $TRPM8_{FA}$ in complex with cooling agents and $PI(4,5)P_2$ [$TRPM8_{FA}$-$PI(4,5)P_2$/icilin/Ca^{2+} and $TRPM8_{FA}$-$PI(4,5)P_2$/WS-12] were reported, providing structural basis for cooling agent and $PI(4,5)P_2$ recognition by TRPM8 and the allosteric coupling between $PI(4,5)P_2$ and cooling agonist [44]. Recently, the great tit bird (*Parus major*) TRPM8 ($TRPM8_{PM}$) structures in complex with inhibitors ($TRPM8_{PM}$-Apo, $TRPM8_{PM}$-AMTB, $TRPM8_{PM}$-TC-I 2014), or Ca^{2+} only ($TRPM8_{PM}$-Ca^{2+}) were published, which suggested the mechanisms of channel inhibition and desensitization [45]. A list of the cryo-EM structures of TRPM8 and TRPV1 that have been published up to date are summarized in Table 1 [40–45].

Overall architectures of the TRPM8 and TRPV1 channels

TRPM8 and TRPV1 form homotetramers consisting of the transmembrane channel domain (TMD) and the cytoplasmic domain (CD) (Figure 1A) [41, 43]. Analogous to the voltage-gated cation channels, the TMDs of TRPM8 and TRPV1 can be divided into a **voltage-sensor-like domain** (**VSLD**) composed of the transmembrane helical segments S1 to S4, and a pore domain formed by S5 and S6 helices and a pore helix (PH) (Figure 1B-D). The TMDs of the homotetrameric channels are arranged in a domain-swapped configuration where the VSLD of one protomer interacts with the pore domain from the neighboring protomer. For both TRPM8 and TRPV1, their CDs comprise the N- and C-terminal domains (NTD and CTD, respectively) and constitute a major proportion of the full-length channels but exhibit significant structural divergences (Figure 1B-D). In TRPM8 channel, the CD comprises the melastatin homology regions 1 to 4 (MHR1 to MHR4), which are characteristic features of members from the TRPM subfamily, and a membrane peripheral pre-S1 domain at the N-terminus, together with the conserved TRP domain followed by two extended CTD helices (CTDH1 and CTDH2) and a coiled-coil (CC) at the C-terminus. In stark contrast, the cytosolic region of the TRPV1 channel is composed of an ankyrin repeat domain (ARD; AR1 to AR6), a linker domain, and a pre-S1 helix at the N-terminus, as well as a TRP domain and a CTD at the C-terminus.

Comparing to TRPV1, TRPM8 exhibits several distinct structural features in the TMD as well as in the domain assembly of CD. First, the transmembrane helices (S1-S6) of the apo TRPM8 structures ($TRPM8_{FA}$-Apo) all adopt **α-helical** configuration (Figure 1E), whereas the TMs in TRPV1-Apo contain non-α-helical elements, such as 3_{10}- and **π-helices**, which have been proposed to provide flexibility and serve critical roles in TRP channel gating (Figure 1G) [46, 47]. In apo TRPM8, the straight α-helical S4 and S5 are connected via a

sharp turn at a conserved proline residue. Notably, subsequent structural studies show that agonist binding induces secondary structure changes in S4 and introduces a bending in S5 (Figure 1F) [44].

Second, different from TRPV channels which contain a single cytosolic pre-S1 helix linking the TMD and the CD, TRPM8 has an expanded pre-S1 domain located at the membrane interface, which is composed of an additional helix and a helix-turn-helix motif, together with the cytosolic pre-S1 helix (Figure 1B to D). It has been shown that this membrane peripheral pre-S1 domain constitutes an interfacial cavity for binding the essential modulator $PI(4,5)P_2$ in TRPM8 channel (see section below) [44]. Previous mutagenesis studies also underscored the importance of the pre-S1 domain in TRPM8 function [32, 48].

Third, substantial intra- and inter-subunit interactions are present in TRPM8. Unlike TRPV1 in which the contact between the TMD and CD is mediated by the TRP domain positioned below the membrane bilayer, the pre-S1 domain in TRPM8 establishes additional interactions at the domain interfaces, thereby enhancing the communication between the TMD and CD. In addition, within the CD of TRPM8, the CTDH2 interacts with the adjacent MHR4 and MRH1/2 domains and tightly associates the top and bottom layer of the CD. The MHR3 and MHR1/2 domains from the neighboring protomers form tight interaction networks at the bottom layer of the cytoplasmic ring. Together, these distinguishing features in the TRPM8 architecture provide the structural basis for its functions.

Distinct binding sites for cooling agonists and vanilloids

Cryo-EM studies have revealed that the cooling agonists and the vanilloid compounds bind to distinct locations in the TMDs of TRPM8 and TRPV1 channels, respectively (Figure 2A) [40, 42, 44]. The vanilloid-binding pocket in the TRPV1 channel was uncovered when the rat TRPV1 structures in complex with DkTx/RTx and capsaicin were captured in amphipol and nanodiscs [40, 42]. It is located above the S4-S5 linker and embraced by S3 and S4 in the VSLD from the same subunit and S6 from the neighboring pore domain (S6’) (Figure 2B). In the absence of vanilloid agonists, phosphatidylinositol (PtdIns) occupies the same pocket and stabilizes the resting state (closed state) of TRPV1 (Figure 2D) as proposed by Gao *et al* [42]. RTx binding displaces the endogenous lipid and facilitates the electrostatic interactions between R557 in S4b and E570 in the S4-S5 linker, therefore couples the S4-S5 linker movement towards S4 and triggers the channel opening (Figure 2C). On the other hand, a competitive vanilloid **antagonist**, capsazepine resides in the same binding pocket without coordinating the salt bridge formed by R557 and E570 in the DkTx/RTx bound TRPV1 structure (Figure 2E).

Before the TRPM8 structure was solved, a large number of functional studies attempted to probe the binding sites for menthol and other cooling compounds in TRPM8 and to decipher the mechanisms of ligand-dependent channel gating. For instance, residues Y745, R842, and Y1005 in mouse TRPM8 (Y745, R841, and Y1004 in $TRPM8_{FA}$; Y736, R832, and Y995 in $TRPM8_{PM}$) have been shown as critical for menthol binding [39]. (Human, mouse, and rat TRPM8 share the same numbering for key residues mentioned in this review). It has also been shown that Y745 is involved in interacting with a TRPM8 inhibitor SKF96365

[49], which further strengthened the importance of this residue in the ligand-dependent activation of TRPM8. In addition, Chuang *et al.* identified residues N799, D802, and G805 as important for icilin sensitivity in rat TRPM8 (N799, D802, and A805 in $TRPM8_{FA}$; N790, D793, and A796 in $TRPM8_{PM}$) [14]. Several mutagenesis and modeling studies predicted that the binding sites for cooling compounds in TRPM8 are analogous to the vanilloid-binding pocket in the TRPV1 channel, which are located at S2-S3 and positioned towards the membrane bilayer [14, 39, 49, 50]. However, the $TRPM8_{FA}$-Apo structure revealed that residues implicated in ligand binding all face the center of the cavity formed by the VSLD and the TRP domain, which we termed the VSLD cavity (Figure 2F) [43]. In the follow-up cryo-EM studies, TRPM8 structures in complex with the cooling agonists, icilin and the menthol analog WS-12 [referred to as $TRPM8_{FA}$-$PI(4,5)P_2$/icilin/Ca^{2+} and $TRPM8_{FA}$-$PI(4,5)P_2$/WS-12] [44] and with the antagonists, AMTB and TC-I 2014 (referred to as $TRPM8_{PM}$-AMTB and $TRPM8_{PM}$-TC-I 2014) [45] further validated the VSLD cavity as a shared binding site for both agonists and antagonists in the TRPM8 channel (Figure 2F). In contrast to the vanilloid agonists that bind to a membrane-facing site in TRPV1, the cooling agonists occupy a discrete binding cavity in TRPM8 formed by the VSLD and the TRP domain, through which the local structural rearrangements in the ligand binding site are transmitted to the pore for channel gating.

In addition, the Ca^{2+} ion, which is required for TRPM8 activation by icilin, but not by menthol, is shown to be coordinated by residues in S2 and S3 (E782, Q785, N799, and D802 in $TRPM8_{FA}$) in the VSLD cavity of the $TRPM8_{FA}$-$PI(4,5)P_2$/icilin/Ca^{2+} structure (Figure 2G) [44]. The structure of Ca^{2+}-bound $TRPM8_{PM}$ confirmed the location of Ca^{2+} in TRPM8 (Figure 2H) [45]. This Ca^{2+}-binding site in TRPM8 is conserved within the TRPM subfamily, as illustrated by cryo-EM structures of TRPM2, TRPM4, and TRPM8 [44, 45, 51–55].

Molecular basis of ligand recognition by TRPM8

Structures of TRPM8 in complex with various agonists and antagonists allowed for many interesting questions about the ligand recognition by TRPM8 to be addressed. First, how does the VSLD cavity accommodate a wide variety of structurally and chemically distinct, both naturally occurring and synthetic, compounds? Close-up comparisons of the VSLD cavity from different ligand bound TRPM8 structures show that residues lining the binding site can adopt different rotamer conformations (Figure 3A) [44, 45]. Most evidently, R842 in S4, Y1005 and R1008 in the TRP domain of mammalian TRPM8 possess great mobility in their side chain configurations (Figure 3B) (R841, Y1004, and R1007 in $TRPM8_{FA}$; R832, Y995, and R998 in $TRPM8_{PM}$), which enable the residues to navigate through distinct chemical moieties from various ligands. Interestingly, R842 has also been shown contributing to the cold sensitivity and the voltage dependence in human TRPM8 [20]. In addition, Y745 in S1 caps the binding site and interacts with cooling agonists (icilin and WS-12) and antagonists (AMTB and TC-I 2014), suggesting the central role of Y745 in the ligand-dependent gating of TRPM8, which is consistent with the previous functional studies [39, 49].

Second, functional characterizations have shown that unlike menthol, icilin requires intracellular Ca^{2+} for TRPM8 activation [7, 14]. Also, a mutation of alanine to glycine in S3 (the mutation A796G in chicken TRPM8 and A805G in $TRPM8_{FA}$) confers icilin sensitivity to avian TRPM8 orthologs. What are the structural bases of icilin/Ca^{2+} recognition by TRPM8? The $TRPM8_{FA}$-$PI(4,5)P_2$/icilin/Ca^{2+} structure has provided clues to this question (Figure 3C-E) [44]. Ca^{2+} coordination induces structural rearrangements in the VSLD cavity which facilitate icilin binding. Moreover, the glycine substitution in S3 is necessary for icilin binding because it confers mobility in S3, which facilitates coordination of Ca^{2+} and also widens the VSLD cavity to accommodate icilin. Different from the α-helical S4 in the apo and antagonist bound TRPM8 structures (Figure 1E), the S4b in the $TRPM8_{FA}$-$PI(4,5)P_2$/icilin/Ca^{2+} structure adopts a **3_{10}-helix**, which results in a register change and rotation of H844 to the center of the VSLD cavity for icilin interaction (Figure 3E). Interestingly, this α-to-3_{10} helical transition in S4b was not observed in $TRPM8_{FA}$-$PI(4,5)P_2$/WS-12. Subsequent functional studies corroborated the involvement of H844 in icilin-dependent $TRPM8_{FA}$ activation, but not in WS-12-dependent $TRPM8_{FA}$ activation [44]. Despite the progress in our understanding of cooling agonist recognition by TRPM8, both agonist-bound structures adopt non-conductive states; thus, it remains unclear how the cooling agonist-induced conformational changes in the VSLD cavity are translated to the channel opening and whether icilin/Ca^{2+} and menthol activate TRPM8 via different conformational pathways in addition to their distinct binding modes.

Additionally, Diver *et al.* reported the Ca^{2+}-bound $TRPM8_{PM}$ structure ($TRPM8_{PM}$-Ca^{2+}) and suggested structural changes for Ca^{2+}-induced channel desensitization [45]. Compared to $TRPM8_{FA}$-$PI(4,5)P_2$/icilin/Ca^{2+}, in the $TRPM8_{PM}$-Ca^{2+} structure, in spite of the bending in S5, the S4b does not transition to a 3_{10}-helix. Instead, it retains an α-helical configuration resembling that in the apo structure (Figure 3F). It is possible that the $TRPM8_{FA}$-$PI(4,5)P_2$/icilin/Ca^{2+} structure adopts a pre-open (sensitized but non-conducting) state whereas the $TRPM8_{PM}$-Ca^{2+} structure represents a desensitized state. Alternatively, because $PI(4,5)P_2$ is absolutely required for TRPM8 function and removal of $PI(4,5)P_2$ results in channel desensitization [15–17, 56], it is also a possibility that the structures represent two different desensitization states, one following channel activation ($TRPM8_{FA}$-$PI(4,5)P_2$/icilin/Ca^{2+}) while the other ($TRPM8_{PM}$-Ca^{2+}) as a result of $PI(4,5)P_2$ depletion. To fully address the mechanisms of ligand-dependent activation, inhibition, and desensitization, structures of TRPM8 in complex with ligand-free, agonist-bound open, antagonist-bound-closed, and agonist-bound desensitized states in the presence of $PI(4,5)P_2$ are required.

Structural basis of the $PI(4,5)P_2$ dependence in TRPM8 function

$PI(4,5)P_2$ is an important signaling phospholipid in the plasma membrane. It has been shown as a critical regulator of many TRP channels, which include the TRPV, TRPM, and TRPC subfamilies [57, 58]. For TRPV1, two seemingly opposite regulatory effects of $PI(4,5)P_2$, both activating and inhibitory, on the channel gating have been reported [59–61]. The cryo-EM structure of TRPV1 reconstituted in nanodiscs reveals the phosphatidylinositol (PtdIns) binding in the same cleft for vanilloids, from which the inhibitory role of $PI(4,5)P_2$ as a competitive antagonist of vanilloids was proposed (Figure 2C and D) [42]. Although it is a plausible model, it remains to be confirmed if $PI(4,5)P_2$ binds to the PtdIns binding

site in TRPV1. Structure of TRPV1 in complex with $PI(4,5)P_2$ is needed to demystify the complex TRPV1 regulation by $PI(4,5)P_2$ [59, 60]. Putative lipid density in the vanilloid-binding pocket was also observed in cryo-EM structures of TRPV2 [46], TRPV3 [62], and TRPV6 [63], but the identity of this density remains to be determined. Interestingly, a recent structure of the constitutively open TRPV5 channel in complex with $PI(4,5)P_2$ reported a $PI(4,5)P_2$ binding site, which is apart from the vanilloid pocket in TRPV1[64].

$PI(4,5)P_2$ is a common positive regulator of channels from the TRPM subfamily, but members have shown different levels of $PI(4,5)P_2$ dependence on channel activation [65]. In particular, extensive studies have shown for TRPM8 channels specifically, $PI(4,5)P_2$ is required as a cofactor for the channel activation by cooling agonists and cold temperatures [15, 16]. At high concentrations, $PI(4,5)P_2$ itself appears to be sufficient to activate the channel, whereas depletion of the endogenous $PI(4,5)P_2$ results in channel desensitization [15–17]. Mutagenesis studies implicated positively charged residues in the TRP domain are involved in $PI(4,5)P_2$ binding [16]. The binding site for $PI(4,5)P_2$ in TRPM8 was recently defined by Yin *et al.* [44]. In contrast to the PtdIns binding in TRPV1, $PI(4,5)P_2$ binds on the opposite side of S4-S5 at an interfacial cavity between the TMD and the top layer of the CD, which is assembled by multiple key subdomains, including the pre-S1 domain, the S4-S5 junction, the TRP domain, and the MHR4 domain from the neighboring subunit (MHR4') (Figure 4A). The inositol 1,4,5-trisphosphate head group forms electrostatic interactions with basic residues including K605 from MHR4', R688 from the pre-S1 domain, R850 at the S4-S5 junction, and R997 in the TRP domain (K605, R688, R851, and R998 in human TRPM8) (Figure 4B). Furthermore, this interfacial cavity can adopt different conformations which enable $PI(4,5)P_2$ binding in both partially and fully engaged modes (Figure 4C and D). The α-to-3_{10} transition in S4b and the bending of S5 not only reposition the R850 sidechain towards the binding site which provides additional electrostatic interactions with the lipid, but also compact the interfacial cavity and enable fully engagement of the $PI(4,5)P_2$ molecule. Notably, in TRPM8, the MHR4' domain forms extensive interfaces with the pre-S1 and MHR4 domains in the neighboring subunit, which are not observed in the TRPM4 and TRPM2 structures [66, 67] (Figure 4E). The distinct arrangements between CD and TMD amongst TRPM2, TRPM4, and TRPM8 lead to differential interfacial cavity structures. Furthermore, the $PI(4,5)P_2$ interacting residue in the MHR4' is conserved only in TRPM8 [44]. These observations may provide the structural basis of different levels of $PI(4,5)P_2$ dependence on channel activation amongst TRPM family members. Alternatively, it suggests a possibility that the interfacial cavity is not a conserved $PI(4,5)P_2$ site in the TRPM family.

Notably, it is well established that cold, menthol, and $PI(4,5)P_2$ are coupled so that increasing concentration of one ligand enhances the channel sensitivity to the other ligands [15, 16]. Rohacs *et al* [16] proposed that $PI(4,5)P_2$ plays a central role in integrating multiple stimuli into TRPM8 gating. What is the structural basis? We postulate that because $PI(4,5)P_2$ binds to the interfacial nexus where all the functionally important regions are located including VSLD (menthol binding site), the TRP domain, the S4-S5 junction, the CD (MHR4'), and the pre-S1 domain, the $PI(4,5)P_2$ binding will enable coupling of all these subdomains (Figure 4D-E). For example, structural studies have provided mechanistic insights into the allosteric coupling between $PI(4,5)P_2$ and cooling agonists, which are

essential to TRPM8 activation [44]. The locations of cooling agonists and $PI(4,5)P_2$ are strategically positioned at the opposite sides of S4b in the VSLD cavity. As such, the binding of $PI(4,5)P_2$ promotes structural rearrangements, i.e. α-to-3_{10} transition in S4b, bending of S5, and engagement of the TRP domain, which are favorable for the binding of cooling agonists, and vice versa, thereby increasing the apparent affinity for each other (Figure 4F). Moreover, $PI(4,5)P_2$ binding engages multiple subdomains, especially including the VSLD and the TRP domain which are part of the VSLD cavity for cooling agonist binding. As a result, $PI(4,5)P_2$ binding appears to couple the CD and TMD. More critically, it enhances the synergistic binding of cooling agonists in the VSLD for the ligand-dependent channel gating. In contrast, the overlapping locations of phospholipids and vanilloids in TRPV1 have implicated the role of phosphatidylinositol as a negative allosteric regulator of the channel (Figure 2C and D) [42]. Taken together, TRPM8 utilizes a novel design of structural allostery for $PI(4,5)P_2$ and cooling agonists binding, which enables effective control of the channel activation.

Regulatory roles of the cytoplasmic domain in TRPM and TRPV channels

The cytoplasmic domains constitute a great proportion of TRPM8 and TRPV1 channel structures, but their functional roles remain mostly unclear. For TRPM8, it has been shown that the channel is inhibited by G-protein coupled bradykinin receptor B_2 (B2R), leading to pain and inflammation [68, 69]. A recent study revealed direct $G\alpha_q$ gating of TRPM8 via binding to R364 and R368 in MHR1/2 and to R470 in MHR3 in the cytoplasmic domain (Figure 5A) [70]. Neutralization of these basic residues abolished TRPM8 inhibition by $G\alpha_q$ and B2R. So far, there has not been any direct structural evidence depicting interactions between the CD of TRPM8 and any channel modulators. Nevertheless, recent cryo-EM studies of TRPM4 and TRPM2 channels have exemplified several locations in the CDs for agonists' and antagonists' actions on TRPM channels (Figure 5B) [52, 66, 67, 71]. Together, these ligand binding sites in the CD and conformational transitions from the CD to the TMD observed in other TRPM channels might suggest potential roles of the cytoplasmic domain in TRPM8 gating.

In contrast, the currently available cryo-EM structures of TRPV1 are poorly resolved at the distal region of the CTDs, which have hindered structural analysis of interactions between the CTD and the N-terminal ARD and have limited understanding of their functional roles in TRPV1 gating. Nevertheless, the recent cryo-EM studies of TRPV3 in a sensitized and a ligand-bound open state ($TRPV3_{K169A}$ and $TRPV3_{K169A\ 2\text{-}APB}$; PDB IDs: 6OT2 and 6OT5) unveiled structures of the distal CTD region and showed a coil-to-helix transition enhancing the inter-subunit interfacial contacts, which induces coupling between CD and TMD, and primes the channel gating (Figure 5C) [72]. Intriguingly, point mutations in the CTD in TRPV3 render the mutant a voltage-activated channel [72]. Because TRPV1 was the only voltage-activated channel amongst TRPV subtypes, and this voltage sensitivity was proposed to play a key role in integrating temperature sensing into TRPV1 polymodal gating [19], these data strongly suggest that this cytoplasmic interface plays an important role in distinct biophysical properties of TRPV channels as proposed in Zubcevic *et al* [72]. Interestingly, comparison with the TRPV3 structures suggests that the TRPV1-Apo structure may adopt a similar sensitized conformation [72], wherein the ARD (AR5) shows

propensity to engage the neighboring distal CTD (Figure 5D and E), suggesting a regulatory role of the CD in TRPV1 gating. Recent studies also suggested regulatory functions of the CTD in TRPV3 thermal gating [73, 74].

Concluding remarks

The cryo-EM studies of TRPM8 have shown distinguishing structural features in its channel architecture and domain assembly [43–45]. Ligand-bound TRPM8 complex structures have revealed a discrete binding site in the VSLD cavity shared by cooling agonists and antagonists, as well as a membrane interfacial cavity for $PI(4,5)P_2$ binding which is strategically located to synergize with the agonist binding for channel activation. In comparison to the vanilloid receptor TRPV1, structural analyses unveil the essential molecular principles that have designed and preserved TRPM8 as *the* menthol receptor (Figure 6). Although the recent progress in TRPM8 structural biology has provided a framework to understand the ligand recognition by TRPM8, many questions are still unanswered (see Outstanding Questions). First and foremost, the mechanism of ligand-dependent channel gating remains to be addressed. More intriguingly, structural and functional characterizations are needed to uncover the underlying mechanisms of temperature sensing in TRPM8 and in other thermosensitive TRP channels.

Acknowledgements:

This work was supported by the National Institutes of Health (R35NS097241 to S.-Y.L.). We are grateful to Gabriel C. Lander and Mengyu Wu for their impressive efforts during our collaborative work on the $TRPM8_{FA}$-Apo structure. We also thank Huanghe Yang and Son C. Le for the collaboration on functional characterization of TRPM8 and Mario J. Borgnia and Allen L. Hsu for their support in cryo-EM screening and data collection. We thank the former Lee lab members Lejla Zubcevic and William F. Borschel who have contributed to our TRPM8 studies.

Glossary

Agonist
a chemical substance that binds to receptors or ion channels and activates their biological functions

Antagonist
a chemical substance that binds to and inhibits the biological functions of receptors or ion channels

Capsaicin
a vanilloid compound extracted from chili peppers, which produces burning and painful sensations. It functions by activating the vanilloid-receptor TRPV1

Desensitization
the phenomenon that receptors or ion channels become unresponsive after prolonged or repeated exposure to activating stimuli

Menthol

an organic compound found in peppermint, which activates the cold-sensitive TRPM8 ion channel and produces cooling sensation in humans

Nanodiscs
self-assembled discoidal lipid bilayers formed by phospholipids and encircling membrane scaffold proteins. It is widely used to reconstitute membrane proteins of interest into an environment resembling the native lipid bilayer and to facilitate structural determination and functional characterization

Phosphatidylinositol 4,5-bisphosphate ($PI(4,5)P_2$)
a key signaling phospholipid in the plasma membrane involved in many cellular signaling pathways, including regulation of ion channel and receptor functions

Voltage-sensor-like domain (VSLD)
the domain formed by transmembrane helix 1 through 4 (S1-S4) in TRP channels. It is structurally analogous to the voltage sensor domain in canonical voltage-gated cation channels. Functionally its role of voltage sensing in TRP channels remains unclear

α-helix
a common secondary structural motif of proteins, in which the backbone hydrogen bonding is formed between the amine group (N-H) of one amino acid and the carbonyl group (C=O) of another amino acid that is four residues apart in sequence

π-helix
a less common motif of protein secondary structure compared to α-helix. The main chain hydrogen bonding is formed between amino acids that are five residues apart in sequence, resulting in insertion of one additional residue in α-helix and formation of a bulge in the backbone

3_{10}-helix
a less common motif of protein secondary structure compared to α-helix. The main chain hydrogen bonding is formed between amino acids that are three residues apart in sequence. Due to the distorted hydrogen binding network, both π-helix and 3_{10}-helix are structurally flexible and energetically costly and play critical roles in functions and gating of many ion channels, including TRP channels

References:

1. Pedersen SF, Owsianik G, and Nilius B, TRP channels: An overview. Cell Calcium, 2005. 38(3): p. 233–252. [PubMed: 16098585]
2. Ramsey IS, Delling M, and Clapham DE, An introduction to TRP channels. Annu Rev Physiol, 2006. 68: p. 619–47. [PubMed: 16460286]
3. Venkatachalam K. and Montell C, TRP Channels. Annual Review of Biochemistry, 2007. 76(1): p. 387–417.
4. Patapoutian A, et al. , ThermoTRP channels and beyond: mechanisms of temperature sensation. Nature Reviews Neuroscience, 2003. 4(7): p. 529–539. [PubMed: 12838328]
5. Bandell M, Macpherson LJ, and Patapoutian A, From chills to chilis: mechanisms for thermosensation and chemesthesis via thermoTRPs. Curr Opin Neurobiol, 2007. 17(4): p. 490–7. [PubMed: 17706410]

6. Caterina MJ, et al. , The capsaicin receptor: a heat-activated ion channel in the pain pathway. Nature, 1997. 389(6653): p. 816–24. [PubMed: 9349813]
7. McKemy DD, Neuhausser WM, and Julius D, Identification of a cold receptor reveals a general role for TRP channels in thermosensation. Nature, 2002. 416(6876): p. 52–8. [PubMed: 11882888]
8. Peier AM, et al. , A TRP channel that senses cold stimuli and menthol. Cell, 2002. 108(5): p. 705–15. [PubMed: 11893340]
9. Bautista DM, et al. , The menthol receptor TRPM8 is the principal detector of environmental cold. Nature, 2007. 448(7150): p. 204–8. [PubMed: 17538622]
10. Colburn RW, et al. , Attenuated cold sensitivity in TRPM8 null mice. Neuron, 2007. 54(3): p. 379–86. [PubMed: 17481392]
11. Dhaka A, et al. , TRPM8 is required for cold sensation in mice. Neuron, 2007. 54(3): p. 371–8. [PubMed: 17481391]
12. Ma S, et al. , Menthol derivative WS-12 selectively activates transient receptor potential melastatin-8 (TRPM8) ion channels. Pak J Pharm Sci, 2008. 21(4): p. 370–8. [PubMed: 18930858]
13. Wei ET and Seid DA, AG-3–5: a chemical producing sensations of cold. J Pharm Pharmacol, 1983. 35(2): p. 110–2. [PubMed: 6131976]
14. Chuang HH, Neuhausser WM, and Julius D, The super-cooling agent icilin reveals a mechanism of coincidence detection by a temperature-sensitive TRP channel. Neuron, 2004. 43(6): p. 859–69. [PubMed: 15363396]
15. Liu B. and Qin F, Functional control of cold- and menthol-sensitive TRPM8 ion channels by phosphatidylinositol 4,5-bisphosphate. J Neurosci, 2005. 25(7): p. 1674–81. [PubMed: 15716403]
16. Rohacs T, et al. , PI(4,5)P2 regulates the activation and desensitization of TRPM8 channels through the TRP domain. Nat Neurosci, 2005. 8(5): p. 626–34. [PubMed: 15852009]
17. Zakharian E, Cao C, and Rohacs T, Gating of transient receptor potential melastatin 8 (TRPM8) channels activated by cold and chemical agonists in planar lipid bilayers. J Neurosci, 2010. 30(37): p. 12526–34. [PubMed: 20844147]
18. Julius D, TRP channels and pain. Annu Rev Cell Dev Biol, 2013. 29: p. 355–84. [PubMed: 24099085]
19. Voets T, et al. , The principle of temperature-dependent gating in cold- and heatsensitive TRP channels. Nature, 2004. 430(7001): p. 748–54. [PubMed: 15306801]
20. Voets T, et al. , TRPM8 voltage sensor mutants reveal a mechanism for integrating thermal and chemical stimuli. Nat Chem Biol, 2007. 3(3): p. 174–82. [PubMed: 17293875]
21. Clapham DE and Miller C, A thermodynamic framework for understanding temperature sensing by transient receptor potential (TRP) channels. Proc Natl Acad Sci U S A, 2011. 108(49): p. 19492–7. [PubMed: 22109551]
22. Baez D, et al. , Gating of thermally activated channels. Curr Top Membr, 2014. 74: p. 51–87. [PubMed: 25366233]
23. Liu B, et al. , TRPM8 is the principal mediator of menthol-induced analgesia of acute and inflammatory pain. Pain, 2013. 154(10): p. 2169–77. [PubMed: 23820004]
24. Brederson JD, Kym PR, and Szallasi A, Targeting TRP channels for pain relief. Eur J Pharmacol, 2013. 716(1–3): p. 61–76. [PubMed: 23500195]
25. Almaraz L, et al. , Trpm8. Handb Exp Pharmacol, 2014. 222: p. 547–79. [PubMed: 24756721]
26. Andrews MD, et al. , Discovery of a Selective TRPM8 Antagonist with Clinical Efficacy in Cold-Related Pain. ACS Med Chem Lett, 2015. 6(4): p. 419–24.
27. Weyer AD and Lehto SG, Development of TRPM8 Antagonists to Treat Chronic Pain and Migraine. Pharmaceuticals (Basel), 2017. 10(2).
28. Horne DB, et al. , Discovery of TRPM8 Antagonist (S)-6-(((3-Fluoro-4-(trifluoromethoxy)phenyl) (3-fluoropyridin-2-yl)methyl)carbamoy l)nicotinic Acid (AMG 333), a Clinical Candidate for the Treatment of Migraine. J Med Chem, 2018. 61(18): p. 8186–8201. [PubMed: 30148953]
29. Premkumar LS and Sikand P, TRPV1: a target for next generation analgesics. Current neuropharmacology, 2008. 6(2): p. 151–163. [PubMed: 19305794]
30. Szallasi A, Cruz F, and Geppetti P, TRPV1: a therapeutic target for novel analgesic drugs? Trends in Molecular Medicine, 2006. 12(11): p. 545–554. [PubMed: 16996800]

31. Carnevale V. and Rohacs T, TRPV1: A Target for Rational Drug Design. Pharmaceuticals (Basel, Switzerland), 2016. 9(3): p. 52.
32. Matos-Cruz V, et al. , Molecular Prerequisites for Diminished Cold Sensitivity in Ground Squirrels and Hamsters. Cell reports, 2017. 21(12): p. 3329–3337. [PubMed: 29262313]
33. Chigurapati S, et al. , Relaxed constraint and thermal desensitization of the cold-sensing ion channel TRPM8 in mammoths. bioRxiv, 2018: p. 397356.
34. Tewksbury JJ and Nabhan GP, Directed deterrence by capsaicin in chillies. Nature, 2001. 412(6845): p. 403–404. [PubMed: 11473305]
35. Jordt S-E and Julius D, Molecular Basis for Species-Specific Sensitivity to “Hot” Chili Peppers. Cell, 2002. 108(3): p. 421–430. [PubMed: 11853675]
36. Zhang F, et al. , Engineering vanilloid-sensitivity into the rat TRPV2 channel. Elife, 2016. 5.
37. Yang F, et al. , Rational design and validation of a vanilloid-sensitive TRPV2 ion channel. Proc Natl Acad Sci U S A, 2016. 113(26): p. E3657–66. [PubMed: 27298359]
38. Kühn FJP, et al. , Contribution of the S5-Pore-S6 Domain to the Gating Characteristics of the Cation Channels TRPM2 and TRPM8. Journal of Biological Chemistry, 2010. 285(35): p. 26806–26814. [PubMed: 20587417]
39. Bandell M, et al. , High-throughput random mutagenesis screen reveals TRPM8 residues specifically required for activation by menthol. Nat Neurosci, 2006. 9(4): p. 493–500. [PubMed: 16520735]
40. Cao E, et al. , TRPV1 structures in distinct conformations reveal activation mechanisms. Nature, 2013. 504(7478): p. 113–8. [PubMed: 24305161]
41. Liao M, et al. , Structure of the TRPV1 ion channel determined by electron cryomicroscopy. Nature, 2013. 504(7478): p. 107–12. [PubMed: 24305160]
42. Gao Y, et al. , TRPV1 structures in nanodiscs reveal mechanisms of ligand and lipid action. Nature, 2016. 534(7607): p. 347–51. [PubMed: 27281200]
43. Yin Y, et al. , Structure of the cold- and menthol-sensing ion channel TRPM8. Science, 2017: p. eaan4325.
44. Yin Y, et al. , Structural basis of cooling agent and lipid sensing by the cold-activated TRPM8 channel. Science, 2019. 363(6430): p. eaav9334.
45. Diver MM, Cheng Y, and Julius D, Structural insights into TRPM8 inhibition and desensitization. Science, 2019. 365(6460): p. 1434–1440. [PubMed: 31488702]
46. Zubcevic L, et al. , Cryo-electron microscopy structure of the TRPV2 ion channel. Nat Struct Mol Biol, 2016.
47. Zubcevic L. and Lee S-Y, The role of π-helices in TRP channel gating. Current Opinion in Structural Biology, 2019. 58: p. 314–323. [PubMed: 31378426]
48. Zheng W, et al. , Direct Binding between Pre-S1 and TRP-like Domains in TRPP Channels Mediates Gating and Functional Regulation by PIP2. Cell Reports, 2018. 22(6): p. 1560–1573. [PubMed: 29425510]
49. Malkia A, et al. , Differential role of the menthol-binding residue Y745 in the antagonism of thermally gated TRPM8 channels. Mol Pain, 2009. 5: p. 62. [PubMed: 19886999]
50. Pedretti A, et al. , Comparative modeling of the quaternary structure for the human TRPM8 channel and analysis of its binding features. Biochim Biophys Acta, 2009. 1788(5): p. 973–82. [PubMed: 19230823]
51. Zhang Z, et al. , Structure of a TRPM2 channel in complex with Ca(2+) explains unique gating regulation. Elife, 2018. 7.
52. Huang Y, et al. , Architecture of the TRPM2 channel and its activation mechanism by ADP-ribose and calcium. Nature, 2018. 562(7725): p. 145–149. [PubMed: 30250252]
53. Wang L, et al. , Structures and gating mechanism of human TRPM2. Science, 2018. 362(6421): p. eaav4809.
54. Yin Y, et al. , Visualizing structural transitions of ligand-dependent gating of the TRPM2 channel. Nature Communications, 2019. 10(1): p. 3740.
55. Autzen HE, et al. , Structure of the human TRPM4 ion channel in a lipid nanodisc. Science, 2018. 359(6372): p. 228–232. [PubMed: 29217581]

56. Yudin Y, et al. , Decrease in phosphatidylinositol 4,5-bisphosphate levels mediates desensitization of the cold sensor TRPM8 channels. The Journal of Physiology, 2011. 589(24): p. 6007–6027. [PubMed: 22005680]
57. Qin F, Regulation of TRP Ion Channels by Phosphatidylinositol-4,5-Bisphosphate, in Transient Receptor Potential (TRP) Channels, Flockerzi V. and Nilius B, Editors. 2007, Springer Berlin Heidelberg: Berlin, Heidelberg. p. 509–525.
58. Rohacs T, Phosphoinositide regulation of TRP channels. Handbook of experimental pharmacology, 2014. 223: p. 1143–1176. [PubMed: 24961984]
59. Cao E, et al. , TRPV1 channels are intrinsically heat sensitive and negatively regulated by phosphoinositide lipids. Neuron, 2013. 77(4): p. 667–79. [PubMed: 23439120]
60. Senning EN, et al. , Regulation of TRPV1 ion channel by phosphoinositide (4,5)-bisphosphate: the role of membrane asymmetry. J Biol Chem, 2014. 289(16): p. 10999–1006. [PubMed: 24599956]
61. Rohacs T, Phosphoinositide regulation of TRPV1 revisited. Pflügers Archiv - European Journal of Physiology, 2015. 467(9): p. 1851–1869. [PubMed: 25754030]
62. Zubcevic L, et al. , Conformational ensemble of the human TRPV3 ion channel. Nat Commun, 2018. in press.
63. McGoldrick LL, et al. , Opening of the human epithelial calcium channel TRPV6. Nature, 2018. 553(7687): p. 233–237. [PubMed: 29258289]
64. Hughes TET, et al. , Structural insights on TRPV5 gating by endogenous modulators. Nature Communications, 2018. 9(1): p. 4198.
65. Rohacs T, Phosphoinositide regulation of TRP channels. Handb Exp Pharmacol, 2014. 223: p. 1143–76. [PubMed: 24961984]
66. Guo J, et al. , Structures of the calcium-activated, non-selective cation channel TRPM4. Nature, 2017. 552(7684): p. 205–209. [PubMed: 29211714]
67. Huang Y, et al. , Ligand recognition and gating mechanism through three ligand-binding sites of human TRPM2 channel. eLife, 2019. 8: p. e50175.
68. Zhang X, et al. , Direct inhibition of the cold-activated TRPM8 ion channel by Gαq. Nature cell biology, 2012. 14(8): p. 851–858. [PubMed: 22750945]
69. Liu L, et al. , $G_{\alpha q}$ Sensitizes TRPM8 to Inhibition by PI(4,5)P_2 Depletion upon Receptor Activation. The Journal of Neuroscience, 2019. 39(31): p. 6067–6080. [PubMed: 31127000]
70. Zhang X, Direct Gαq Gating Is the Sole Mechanism for TRPM8 Inhibition Caused by Bradykinin Receptor Activation. Cell Reports, 2019. 27(12): p. 3672–3683.e4. [PubMed: 31216483]
71. Winkler PA, et al. , Electron cryo-microscopy structure of a human TRPM4 channel. Nature, 2017. 552(7684): p. 200–204. [PubMed: 29211723]
72. Zubcevic L, et al. , Regulatory switch at the cytoplasmic interface controls TRPV channel gating. eLife, 2019. 8: p. e47746.
73. Singh AK, et al. , Structural basis of temperature sensation by the TRP channel TRPV3. Nature Structural & Molecular Biology, 2019. 26(11): p. 994–998.
74. Macikova L, et al. , Cytoplasmic Inter-Subunit Interface Controls Use-Dependence of Thermal Activation of TRPV3 Channel. Int J Mol Sci, 2019. 20(16).

Outstanding questions:

- What are the mechanisms of ligand-dependent channel activation in TRPM8? How does agonist binding in the voltage-sensor-like domain (VSLD) cavity translate to opening of the pore domain? Do different cooling agonists, such as menthol and icilin, share the same or adopt distinct gating mechanism(s)?
- Agonists and antagonists occupy a common binding site in the VSLD cavity of TRPM8 channel. What are the molecular determinants that enable TRPM8 to differentiate between agonist and antagonist binding which impose opposing effects on channel gating?
- How does TRPM8 detect and sense cold temperatures? Is the molecular mechanism underlying cold sensing by TRPM8 distinct from the principle of heat sensing by TRPV1 and other heat-activated TRP channels?
- What regulatory roles does the cytoplasmic domain serve in TRPM8 channel function? Is it involved in temperature sensation?
- TRPM8 is a polymodal ion channel regulated by cold, cooling agonist, phospholipid, and membrane voltage. How are these physical and chemical stimuli integrated or allosterically coupled to enhance the channel activation? How can we dissect the polymodality in TRPM8 gating?
- TRPM8 is involved in cold hypersensitive in response to tissue inflammation or nerve injuries. How is TRPM8 modulated by inflammatory agents and how does it crosstalk with other signaling pathways in nociception? How can researchers improve and develop pharmacological tools targeting this channel on the basis of structural and mechanistic characterization of TRPM8?

Highlights:

- The transient receptor potential (TRP) channel superfamily members TRPM8 and TRPV1 are two well-known somatosensory receptors that can be activated by both thermal stimuli and natural chemicals
- TRPM8 is the cold and menthol receptor while TRPV1 is the heat and capsaicin receptor in human
- Recent cryo-electron microscopy (cryo-EM) studies of TRPM8 have revealed remarkable structural features that underlie its distinguishing functions in cooling compound sensing, making it unique compared to TRPV1 and other TRP channel members
- These studies also revealed how phosphatidylinositol 4,5-bisphosphate [$PI(4,5)P_2$], which is required for TRPM8 function, binds to a membrane interfacial cavity where functionally important subdomains are localized, and synergizes with the cooling agonist binding for channel activation

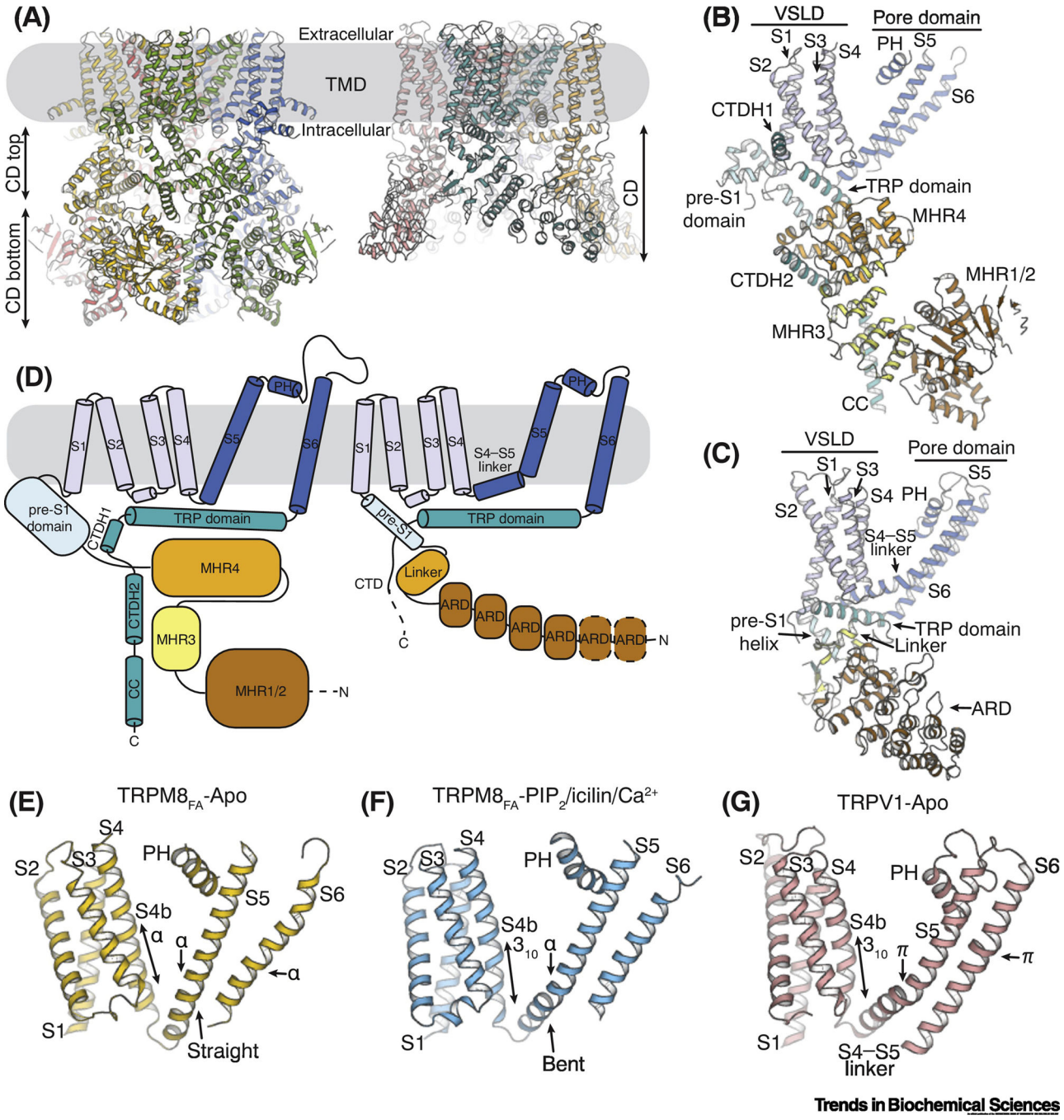

Figure 1. Unique structural features of TRPM8.

(A) Structure models showing the architecture of TRPM8 (left; PDB ID: 6BPQ) and TRPV1 (right; PDB ID: 3J5P) channels. The transmembrane domains (TMDs) are embedded in the plasma membrane (gray box). The cytoplasmic domain (CD) of TRPM8 can be further divided into the top (CD top) and the bottom (CD bottom) layers.

(B and C) Atomic models of a single protomer from TRPM8 (B) and TRPV1 (C), respectively. Abbreviations: ARD, ankyrin repeat domain; CC, coiled coil; CTDH, C-

terminal domain helix; MHR, melastatin homology region; PH, pore helix; VSLD, voltage-sensor-like domain.

(D) Cartoon diagrams delineating the topology of TRPM8 (left) and TRPV1 (right). Subdomains labeled as in B and C.

(E-G) Comparison of the transmembrane domain (TMD) in the apo $TRPM8_{FA}$ (E,; PDB ID: 6BPQ), $TRPM8_{FA}$ in complex with $PI(4,5)P_2$/icilin/Ca^{2+} (F; PDB ID: 6NR3), and the apo TRPV1 structures (G; PDB ID: 3J5P). The configurations of secondary structure in the C-terminus of S4 (S4b), S5, and S6 are indicated by arrows for comparison.

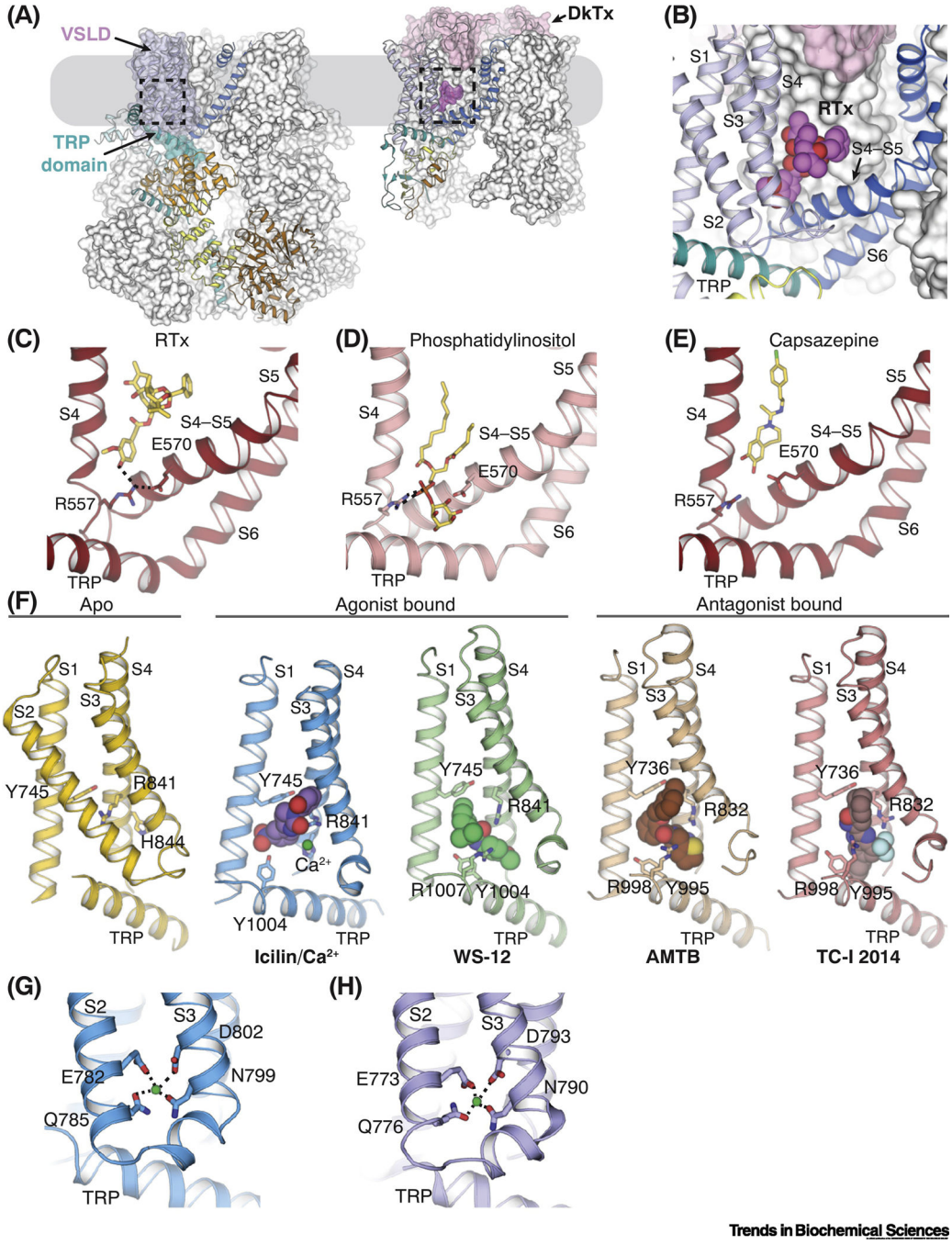

Figure 2. The novel binding site for agonists and antagonists in TRPM8.

(**A**) The locations of ligand binding in TRPM8 (left) and TRPV1 (right) embedded in the plasma membrane (gray box), which are highlighted by dashed lines. The ligand binding site in TRPM8 is located in the voltage-sensor-like domain cavity (VSLD cavity) formed by the VSLD and the TRP domain. The double-knot toxin (DkTx, pink surface representation) binds atop TRPV1 channel. For each channel, one protomer is shown as in Figure 1B and C, while the rest are shown in white surface representation.

(**B**) Close-up view of the binding site for resiniferatoxin (RTx) in TRPV1. Magenta spheres represent the RTx molecule.

(C-E) Comparison of the binding of vanilloid agonist RTx (C; PDB ID: 5IRX), phosphatidylinositol lipid (D; PDB ID: 5IRZ), and antagonist capsazepine (E; PDB ID: 5IS0) in TRPV1 channel. Dashed lines indicate interactions mediated by R557 in S4 and E570 in S4-S5 linker. Ligands are shown as sticks.

(F) Comparison of the VSLD cavity in the ligand-free $TRPM8_{FA}$ (yellow; PDB ID: 6BPQ), $TRPM8_{FA}$-$PI(4,5)P_2$/icilin/Ca^{2+} complex (blue; PDB ID: 6NR3), $TRPM8_{FA}$-$PI(4,5)P_2$/WS-12 complex (green; PBD ID: 6NR2), $TRPM8_{PM}$-AMTB complex (wheat; PDB ID: 6O6R), and $TRPM8_{PM}$-TCI-2014 complex (pink; PDB ID: 6O72). Key residues for ligand binding are shown in sticks. Spheres represent agonists, antagonists, and Ca^{2+} ion. In panels for ligand-bound structures, S2 is omitted for clarity.

(G-H) Ca^{2+} binding in the VSLD cavity of $TRPM8_{FA}$-$PI(4,5)P_2$/icilin/Ca^{2+} (G) and $TRPM8_{PM}$-Ca^{2+} (H; PDB ID: 6O77) complex structures. Green spheres represent Ca^{2+} ions. Dashed lines indicate the ion coordination.

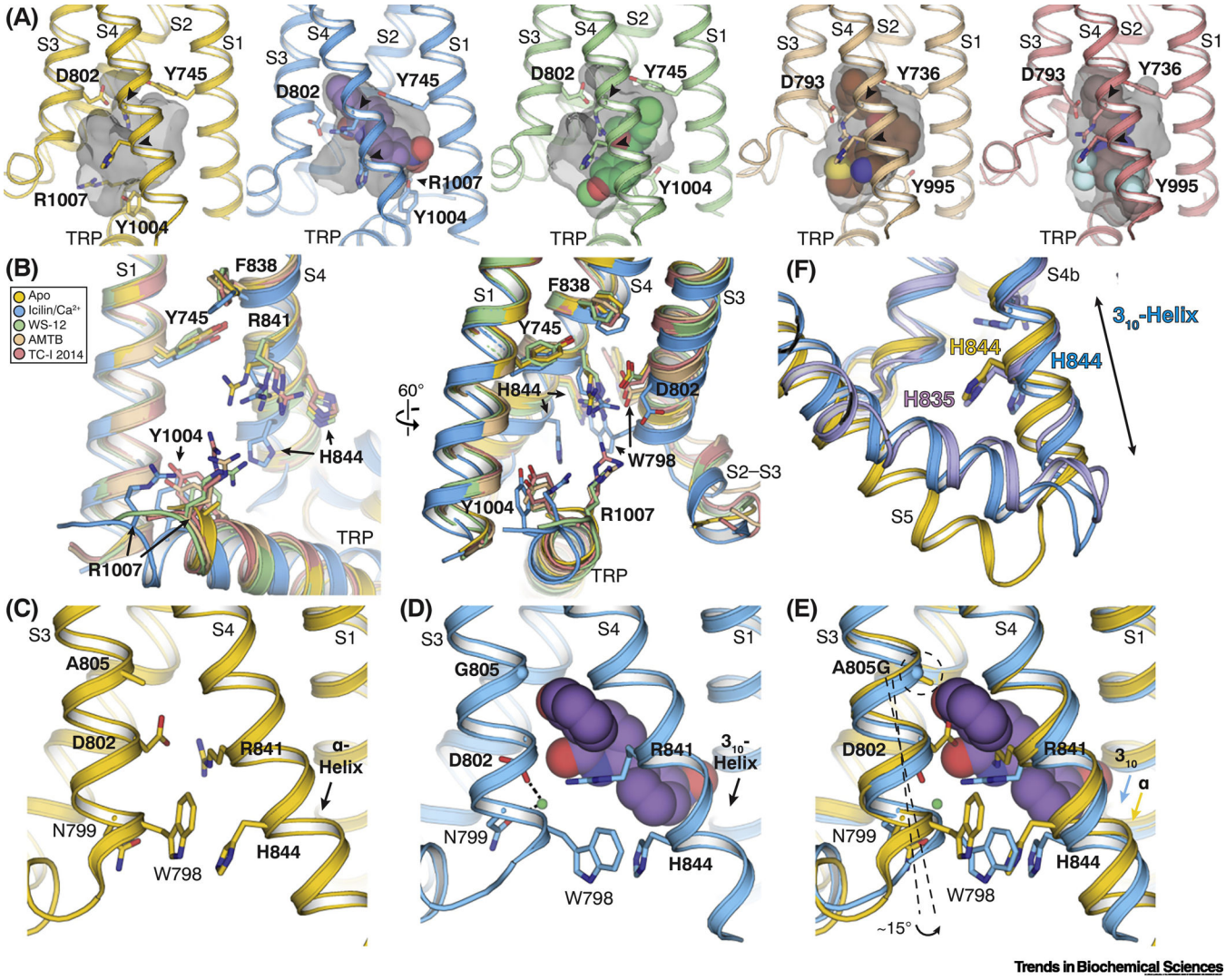

Figure 3. Molecular basis of ligand recognition by TRPM8.

(A) Comparison of the VSLD cavity in the $TRPM8_{FA}$-Apo (yellow), $TRPM8_{FA}$-$PI(4,5)P_2$/icilin/Ca^{2+} complex (blue), $TRPM8_{FA}$-$PI(4,5)P_2$/WS-12 complex (green), $TRPM8_{PM}$-AMTB complex (wheat), and $TRPM8_{PM}$-TC-I 2014 complex (pink). Gray transparent surfaces represent the shape of the cavity mediated by residues lining the binding pocket. Arrowheads point the flexible arginine and histidine residues in S4 (R841 and H844 in $TRPM8_{FA}$; R832 and H835 in $TRPM8_{PM}$). Ligands are shown in spheres. PDB IDs indicated in Figure 2F legend.

(B) Overlay of the VSLD cavity in the ligand bound TRPM8 structures, showing the flexibility of the key ligand-binding residues. Color coding is the same as in (A). Residue numbering refers to $TRPM8_{FA}$.

(C-E) Comparison of the VSLD cavity in the $TRPM8_{FA}$-Apo (C, yellow) and the $TRPM8_{FA}PI(4,5)P_2$/icilin/Ca^{2+} complex (D, blue) structures, showing the conformational changes induced by icilin (purple spheres) and Ca^{2+} (green sphere) binding; especially S4b undergoes a α-to-3_{10} helical transition. Superimposition of the two structures (E) suggests the Ca^{2+} coordination facilitates the icilin binding; the A805G mutation confers flexibility in

S3 for the assembly of Ca^{2+} coordination and widens the VSLD cavity to accommodate the icilin molecule.

(F) Comparison of the ligand-induced conformational changes in S4 and S5 between $TRPM8_{FA}$-$PI(4,5)P_2$/icilin/Ca^{2+} (blue) and $TRPM8_{PM}$-Ca^{2+} structures (purple) with $TRPM8_{FA}$-Apo (yellow). Ligand binding induces bending of S5 in $TRPM8_{FA}$-$PI(4,5)P_2$/icilin/Ca^{2+} (blue) and $TRPM8_{PM}$-Ca^{2+}. The S4b in $TRPM8_{PM}$-Ca^{2+} remains α-helical, whereas that in $TRPM8_{FA}$-$PI(4,5)P_2$/icilin/Ca^{2+} transitions to a 3_{10}-helix.

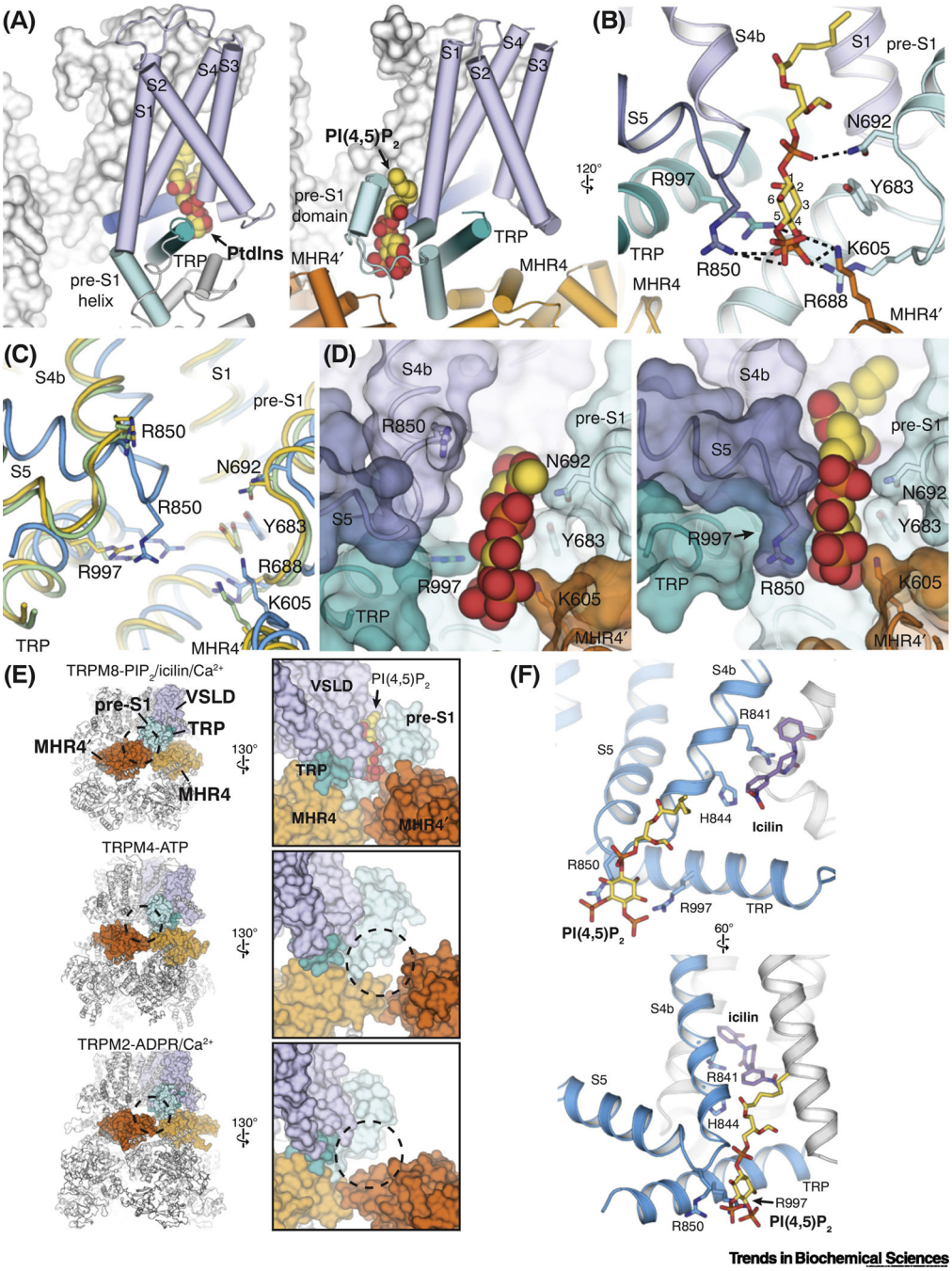

Figure 4. Structural basis of the PI(4,5)$_2$ dependence of TRPM8.

(**A**) Comparison of the binding site for phosphatidylinositol lipid (PtdIns) (left; PDB ID: 5IRZ) in TRPV1 and that for PI(4,5)P_2 in TRPM8 (right; PDB ID: 6NR3). Lipid molecules are shown as spheres.

(**B**) Residues interacting with PI(4,5)P_2 (yellow sticks) in the interfacial cavity in TRPM8.

(**C**) Comparison of the PI(4,5)P_2 binding site in TRPM8$_{FA}$-Apo (yellow), TRPM8$_{FA}$-PI(4,5)P_2/icilin/Ca^{2+} complex (blue), and TRPM8$_{FA}$-PI(4,5)P_2/WS-12 complex (green).

Structural rearrangements of S4 and S5 in the $TRPM8_{FA}$-$PI(4,5)P_2$/icilin/Ca^{2+} complex reposition R850 closer to the $PI(4,5)P_2$ binding site. PDB IDs indicated in Figure 2F legend.
(**D**) Surface representations showing two different conformations of the interfacial cavity which enable partially (left, $TRPM8_{FA}$-$PI(4,5)P_2$/WS-12 complex) and fully (right, $TRPM8_{FA}$-$PI(4,5)P_2$/icilin/Ca^{2+} complex) engagement of $PI(4,5)P_2$ with the TRPM8 channel. $PI(4,5)P_2$ is shown in spheres.
(**E**) Global (left columns) and close-up (right columns) views comparing the intra- and inter-subunit domain interfaces in TRPM8 (PDB ID: 6NR3), TRPM4 (PDB ID: 5WP6), and TRPM2 (PDB ID: 6PUS). Tight association between the pre-S1 domain and the neighboring MHR4 domains contributes to the $PI(4,5)P_2$ binding site in TRPM8.
(**F**) Distinct but adjacent binding sites for $PI(4,5)P_2$ (yellow sticks) and icilin (purple sticks) (PDB ID: 6NR3) illustrate the allosteric coupling between the lipid and cooling agonists for TRPM8 activation.

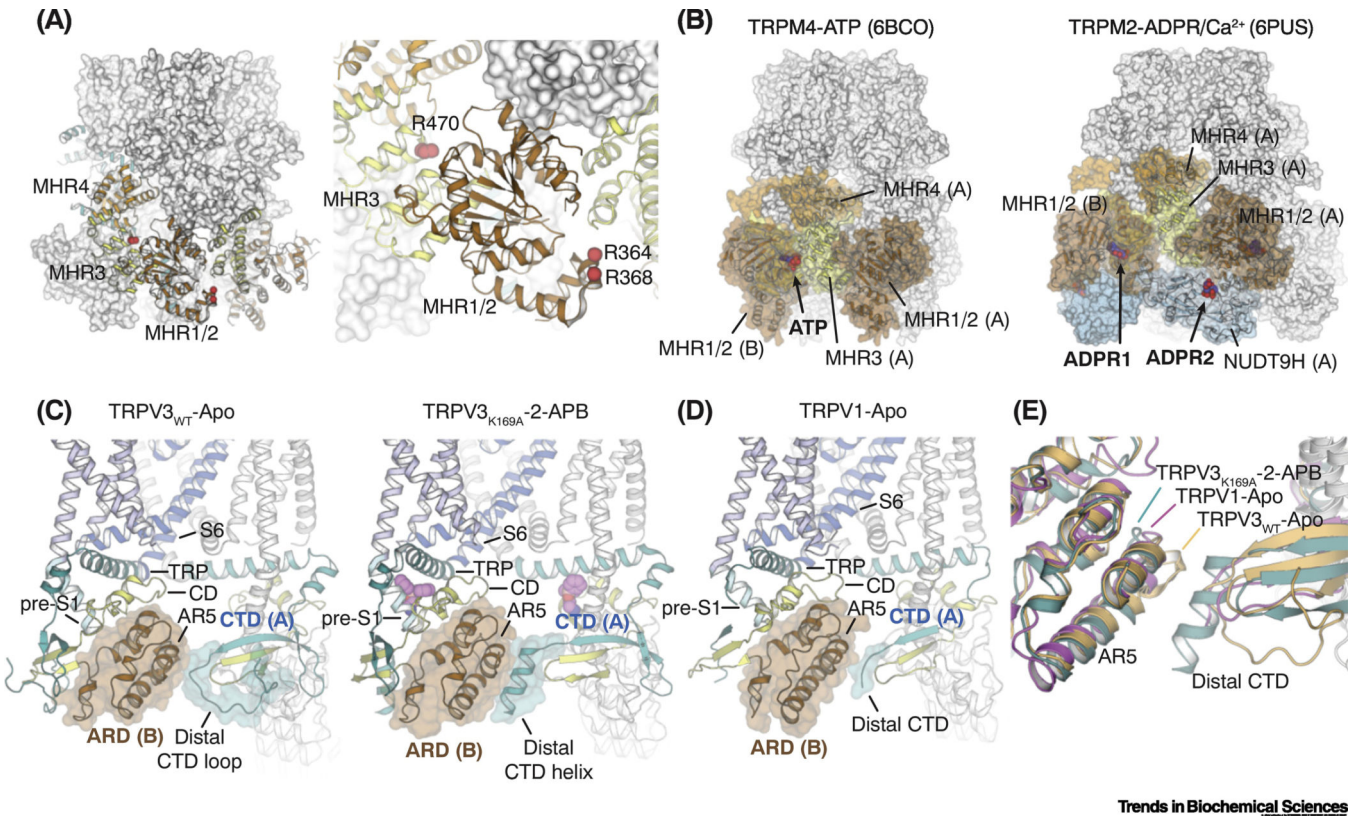

Figure 5. Regulatory functions of cytoplasmic domains in TRPM and TRPV channels.

(A) Residues in TRPM8 (red spheres) that have been implicated for direct interactions with $G\alpha_q$ mapped to the MHR1/2 and MHR3 domains.

(B) The ligand binding sites for ATP in TRPM4 (left; PDB ID: 6BCO) and ADP-ribose (ADPR) in TRPM2 (right; PDB ID: 6PUS) are located in the cytoplasmic domains of the channel.

(C) In TRPV3, state-dependent secondary structure changes from loop (left; PDB ID: 6MHO) to helix (right; PDB ID: 6OT5) in the distal C-terminal domain (CTD) triggers rearrangements in the inter-subunit interfaces, which are propagated to the TRP domain and lead to channel activation.

(**D**) Inter-subunit interface between the distal CTD and the neighboring ankyrin repeat domain (ARD) in the TRPV1-Apo structure (PDB ID: 3J5P).

(**E**) Structural comparison of the less-well defined CTD and ARD in the TRPV1-Apo with those in the closed and the open states of TRPV3. $TRPV3_{WT}$-Apo: light orange, PDB 6MHO; $TRPV3_{K169A}$-2-APB: teal, PDB 6OT5; TRPV1-Apo: magenta, PDB 3J5P.

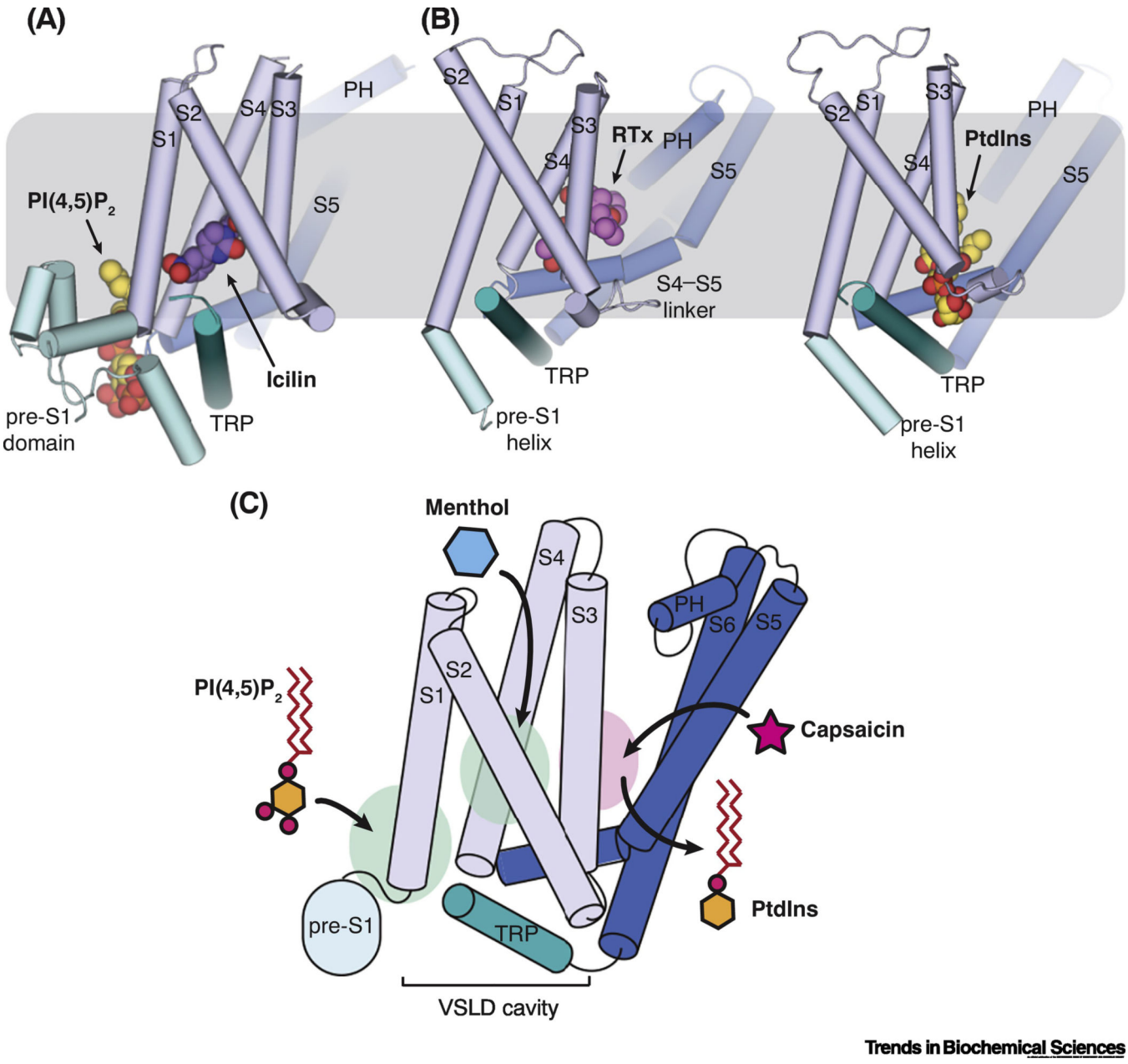

Figure 6. The design principle of synergetic actions of PI(4,5)P_2 and cooling agonists on TRPM8 activation.

(A and B) Comparison of the distinct binding sites for lipid and agonists in TRPM8 (A) and TRPV1 (B) channels. The gray box represents the plasma membrane. Cytoplasmic domains of the channels are simplified.

(C) Schematic diagram depicting a discrete binding site for menthol in the VSLD cavity and the strategic position of PI(4,5)P_2 binding for allosteric coupling with cooling agonist in TRPM8. In contrast, capsaicin and membrane lipid share the same binding pocket above the S4-S5 linker in TRPV1, where PtdIns is proposed to act as a competitive antagonist for vanilloid activation based on the structure. The locations representative of ligand binding in

TRPM8 and TRPV1 are shown as green and pink ovals, respectively. Cytoplasmic domains are omitted for simplicity.

Table 1

A summary of the published cryo-EM structures of TRPV1 and TRPM8 channels.

Channel	Ligand	Biochemical condition	Structure annotation	Resolution	PDB ID	Reference
TRPV1	Apo	Amphipol	TRPV1-Apo	3.4 Å	3J5P	[41]
	DkTx/RTx	Amphipol	TRPV1-DkTx/RTx	3.8 Å	3J5Q	[40]
	Capsaicin	Amphipol	TRPV1-Capsaicin	4.2 Å	3J5R	
	Apo	Lipid nanodiscs	$TRPV1_{ND}$-Apo	3.28 Å	5IRZ	[42]
	DkTx/RTx	Lipid nanodiscs	$TRPV1_{ND}$-DkTx/RTx	2.95 Å	5IRX	
	Capsazepine	Lipid nanodiscs	$TRPV1_{ND}$-Capsazepine	3.43 Å	5IS0	
$TRPM8_{FA}$	Apo	Detergent	$TRPM8_{FA}$-Apo	4.1 Å	6BPQ	[43]
	$PI(4,5)P_2$/icilin/Ca^{2+}	Detergent	$TRPM8_{FA}$-$PI(4,5)P_2$/icilin/Ca^{2+} class 1	3.4 Å	6NR3	[44]
			$TRPM8_{FA}$-$PI(4,5)P_2$/icilin/Ca^{2+} class 2	4.3 Å	6NR4	
	$PI(4,5)P_2$/WS-12	Detergent	$TRPM8_{FA}$-$PI(4,5)P_2$/WS-12	4.0 Å	6NR2	
$TRPM8_{PM}$	Apo	Amphipol	$TRPM8_{PM}$-Apo	3.6 Å	6O6A	[45]
	AMTB	Amphipol	$TRPM8_{PM}$-AMTB	3.2 Å	6O6R	
	TC-I 2014	Amphipol	$TRPM8_{PM}$-TC-I 2014	3 Å	6O72	
	Ca^{2+}	Amphipol	$TRPM8_{PM}$-Ca^{2+}	3.2 Å	6O77	